Numerical and Parametric Investigation on the Dynamic Response of a Planar Multi-body System with Differently Located Revolute Clearance Joints

Onesmus Muvengei, John Kihiu and Bernard Ikua

Abstract—As a step towards the investigation of dynamic interaction of revolute clearance joints in a multi-body mechanical system, this paper numerically investigates the parametric effects of differently located revolute clearance joints without friction on the overall dynamic characteristics of a multi-body system. A typical planar slider-crank mechanism is used as a demonstration case in which the parametric effects of a revolute clearance joint between the crank and connecting rod, and between the connecting rod and slider are separately investigated with comprehensive observations numerically presented. The selected parameters are the clearance size and the input crank speed. It is observed that, different joints in a multi-body system have different sensitivities to the clearance size, and changing the driving speed of a mechanism makes the behavior of the mechanism to change from either periodic to chaotic, or chaotic to periodic depending on which joint has clearance. Therefore the dynamic behavior of one clearance revolute joint cannot be used as a general case for a mechanical system. Also the location of the clearance revolute joint, the clearance size and the operating speed of a mechanical system, play a crucial role in predicting accurately the dynamic responses of the system.

Keywords—Chaotic behavior, Contact-impact forces, Dynamic response, Multi-body mechanical system, Periodic behavior, Poincaré maps, Quasi-periodic behavior, Revolute clearance joint

I. Introduction

THE dynamic modeling of multi-body systems is a key aid in the analysis, design, optimization, control, and simulation of mechanisms and manipulators. However, clearance, friction, impact and other phenomena associated with real joints have been routinely ignored in order to simplify the dynamic model. The increasing requirement for high-speed and precise machines, mechanisms and manipulators demands that the kinematic joints be treated in a realistic way. This is because in a real mechanical joint, a clearance which permits the relative motion between the connected bodies as well as the components assemblage, is always present. The clearance no matter how small it is, can lead to vibration and fatigue phenomena, premature failure and lack of precision or even random overall behavior.

There is a significant amount of literature available which discuses theoretical and experimental analysis of imperfect kinematic joints in a variety of planar and spatial mechanical systems with rigid or flexible links [1]–[37]. Many of these works focus on the planar systems in which only one kinematic joint is modeled as an imperfect joint [1], [2], [4]–[13], [15]–[18], [20]–[23], [26], [27], [30]–[35]. Although, the results from such experimental and analytical models have been shown to provide important insights on the behavior of mechanical systems with imperfect joints, the models do not allow for study of the interactions of multiple kinematic imperfect joints. Furthermore a real mechanical system does not have only one real joint, but practically all joints are real. This led several researchers such as Flores (2004) [38] and Cheriyan (2006) [39] to strongly recommend for their work to be extended to include multi-body mechanical systems with multiple imperfect joints, and with a variety of joints such as prismatic and universal joints. Few recent papers by Erkaya and Uzmay (2009-2010) [19], [25], and by Flores (2010) [36] have considered the nonlinear dynamic analysis of multi-body systems with two imperfect joints. However in these research papers, only mechanisms with rigid links have been considered and the interaction effects of the imperfect joints on the overall response of a multi-body system were not investigated. Also, Erkaya and Uzmay (2009-2010) [19], [25] modeled the clearance in the journal bearing as a massless imaginary link whose length is equal to the clearance size. This assumption is not valid especially at large clearances because the journal and bearing will not be in contact at all times.

The primary objective of this research work therefore is to numerically quantify the influence of the main parameters on the dynamic characteristics of a rigid-planar multi-body mechanical system with differently located revolute clearance joints without friction. The selected parameters are the clearance size and the input crank speed. This work will provide inherent information which can be of great use in the analysis of multi-body systems with clearance joints especially as it regards to the effective design and control tasks of these systems. This study will also form a base towards the investigation of dynamic interaction of multiple revolute clearance joints in a multi-body mechanical system.

II. Equations of Motion of Multi-body Systems

In order to analyze the dynamic response of a multi-body system whether with ideal or real joints, it is first necessary to formulate the equations of motion that govern its behavior. The process of formulating the equations which govern the behavior of the system is called modeling the system, while the process of numerically solving the generated equations of

O. Muvengei, is an Assistant Lecturer in the Department of Mechanical Engineering, JKUAT (+254720642441; e-mail: ommuvengei@gmail.com).

J. Kihiu, is an Associate Prof in the Department of Mechanical Engineering, JKUAT (e-mail: kihiusan@yahoo.com).

B. Ikua, is a Senior Lecturer in the Department of Mechatronic Engineering, JKUAT (e-mail: ikua-bw@eng.jkuat.ac.ke).

motion in order to analyze the system's response is termed as simulation.

In computational kinematic and dynamic analysis of multi-body mechanical systems, a set of algebraic kinematic constraint equations which describe the joint connectivity between the bodies of the multi-body system are used. These kinematic constraint equations can be presented in terms of appropriate system of coordinates which allow one to clearly define at all times the position, velocity and acceleration of all bodies of the mechanical system.

The kinematic constraints considered in this work are assumed to be holonomic (geometric constraints), that is, constraints which are expressed as functions of the coordinates and, possibly, time. If the time does not appear explicitly in a constraint equation, then the system is said to be scleronomic. A simple example of scleronomic constraint equations is the revolute joint between any two bodies in a four-bar mechanism. Otherwise, when the constraint is holonomic and time appears explicitly, the system is said to be rheologic. A simple example of rheologic constraint equation is the driving constraint in kinematically driven mechanism.

The methodology adopted in this work to derive the dynamic equations of multi-body systems follows closely that of Nikravesh (1988) [40], in which the generalized Cartesian coordinates and the Newton-Euler's approach are utilized. In addition, the Baumgarte stabilization technique [41] is used to control the position and velocity violations during direct integration of the equations of motion. The methodology presented is implemented in a MATLAB code, which is capable of automatically generating and solving the equations of motion for the multi-body systems.

Computational kinematic analysis of a multi-body system is performed by solving the set of equations 2, 4 and 6 for q, $\dot{q}$ and $\ddot{q}$ respectively. This formulation can be implemented on a computer code, and made available for kinematic analysis of a large class of multi-body mechanical systems.

Position Analysis: The constraint equations vector can be written as,

$$C(\mathbf{q},t)=\Big[C_1(\mathbf{q},t)\;\; C_2(\mathbf{q},t).....C_n(\mathbf{q},t)\Big]^T = 0 \qquad (1)$$

This equation contains n nonlinear scalar equations which can be solved for the n unknown generalized coordinates given in a vector form as,

$$\mathbf{q} \;=\; \Big[\mathbf{q_1}\;\; \mathbf{q_2}\;\; \mathbf{q_3}\;\; .....\mathbf{q_n}\Big]^T$$

Newton-Raphson iteration procedure was used in this work to solve this set of nonlinear algebraic equations. This algorithm involves linearizing the set of nonlinear equations of kinematic constraints to get the first order approximation of equation $C(\mathbf{q},t)=0$ as,

$$C_{q_i}\Delta q_i \;=\; -C(\mathbf{q}_i,t) \qquad (2)$$

where,

(a) C_{q_i} is the Jacobian matrix at iteration point *i*, given as,

$$C_{q_i} \;=\; \begin{pmatrix} \frac{\partial C_1}{\partial q_1} & \frac{\partial C_1}{\partial q_2} & \frac{\partial C_1}{\partial q_3}..... & \frac{\partial C_1}{\partial q_n} \\ \frac{\partial C_2}{\partial q_1} & \frac{\partial C_2}{\partial q_2} & \frac{\partial C_2}{\partial q_3}..... & \frac{\partial C_2}{\partial q_n} \\ \frac{\partial C_3}{\partial q_1} & \frac{\partial C_3}{\partial q_2} & \frac{\partial C_3}{\partial q_3}..... & \frac{\partial C_3}{\partial q_n} \\ . & . & . & . \\ . & . & . & . \\ \frac{\partial C_n}{\partial q_1} & \frac{\partial C_n}{\partial q_2} & \frac{\partial C_n}{\partial q_3}..... & \frac{\partial C_n}{\partial q_n} \end{pmatrix} \qquad (3)$$

For kinematically driven system, the Jacobian matrix is a square non-singular matrix.

(b) Δq_i is the vector of Newton differences at iteration point *i*

(c) $C(\mathbf{q}_i,t)$ is the vector of constraint equations at iteration point *i*.

Velocity Analysis: This involves solving linear equation 4 for $\dot{q}$

$$C_q\dot{q} \;=\; -C_t \qquad (4)$$

where C_q is the constraint Jacobian matrix given by equation 3 and C_t is the vector of partial derivatives of the constraint equations with respect to time, which is given as,

$$C_t \;=\; \Big[\;\frac{\partial C_1}{dt}\;\;\frac{\partial C_2}{dt}\;\;\frac{\partial C_3}{dt}.....\;\;\frac{\partial C_n}{dt}\;\Big]^T \qquad (5)$$

Acceleration Analysis: This involves solving linear equation 6 for $\ddot{q}$

$$C_q\ddot{q} \;=\; -(C_q\dot{q})_q\dot{q} - 2C_{qt}\dot{q} - C_{tt} \qquad (6)$$

where

(a) C_{qt} is the time derivative of the Jacobian matrix given as,

$$C_{qt}=\begin{pmatrix} \frac{\partial}{\partial t}\Big[\frac{\partial C_1}{\partial q_1}\Big] & \frac{\partial}{\partial t}\Big[\frac{\partial C_1}{\partial q_2}\Big] & \frac{\partial}{\partial t}\Big[\frac{\partial C_1}{\partial q_3}\Big]..... & \frac{\partial}{\partial t}\Big[\frac{\partial C_1}{\partial q_n}\Big] \\ \frac{\partial}{\partial t}\Big[\frac{\partial C_2}{\partial q_1}\Big] & \frac{\partial}{\partial t}\Big[\frac{\partial C_2}{\partial q_2}\Big] & \frac{\partial}{\partial t}\Big[\frac{\partial C_2}{\partial q_3}\Big]..... & \frac{\partial}{\partial t}\Big[\frac{\partial C_2}{\partial q_n}\Big] \\ \frac{\partial}{\partial t}\Big[\frac{\partial C_3}{\partial q_1}\Big] & \frac{\partial}{\partial t}\Big[\frac{\partial C_3}{\partial q_2}\Big] & \frac{\partial}{\partial t}\Big[\frac{\partial C_3}{\partial q_3}\Big]..... & \frac{\partial}{\partial t}\Big[\frac{\partial C_3}{\partial q_n}\Big] \\ . & . & . & . \\ . & . & . & . \\ \frac{\partial}{\partial t}\Big[\frac{\partial C_n}{\partial q_1}\Big] & \frac{\partial}{\partial t}\Big[\frac{\partial C_n}{\partial q_2}\Big] & \frac{\partial}{\partial t}\Big[\frac{\partial C_n}{\partial q_3}\Big]..... & \frac{\partial}{\partial t}\Big[\frac{\partial C_n}{\partial q_n}\Big] \end{pmatrix} \qquad (7)$$

(b) C_{tt} is the vector of second partial derivatives of the constraint equations with respect to time, which is given as,

$$C_{tt} \;=\; \Big[\;\frac{\partial^2 C_1}{dt^2}\;\;\frac{\partial^2 C_2}{dt^2}\;\;\frac{\partial^2 C_3}{dt^2}.....\;\;\frac{\partial^2 C_n}{dt^2}\;\Big]^T \qquad (8)$$

The computational scheme for the kinematic analysis of mechanical systems which consist of interconnected rigid bodies is as shown in Figure 1.

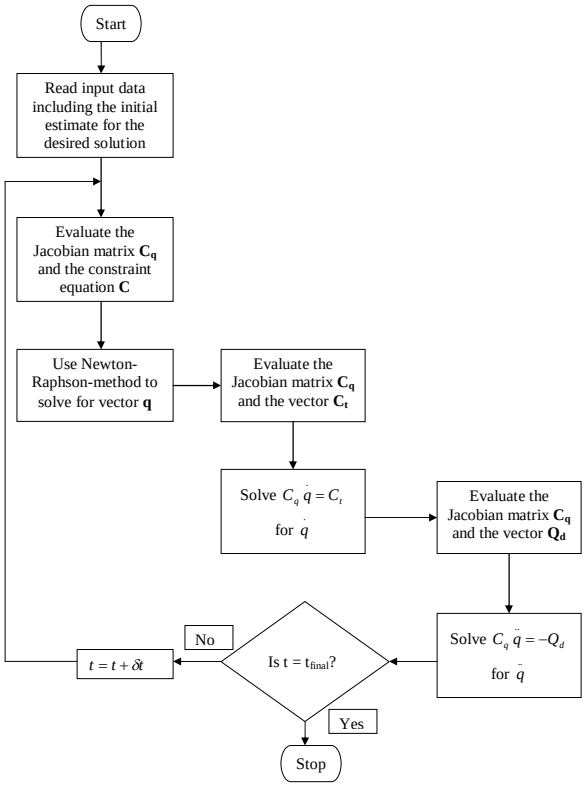

Fig. 1. Flowchart of computational procedure for kinematic analysis of a multi-body system

Computationally, the dynamic analysis of a multi-body mechanical system involves solving equation 9 numerically for $\ddot{\mathbf{q}}$ and λ [42]. Then, in each integration time step, the accelerations vector, $\ddot{\mathbf{q}}$, together with velocities vector, $\dot{\mathbf{q}}$ are integrated in order to obtain the system velocities and positions for the next time step. This procedure is repeated until the final analysis time is reached.

$$\begin{pmatrix} M & C_q^T \\ C_q & 0 \end{pmatrix} \begin{pmatrix} \ddot{q} \\ \lambda \end{pmatrix} = \begin{pmatrix} Q_e \\ -(C_q \dot{q})_q \dot{q} - 2C_{qt}\dot{q} - C_{tt} \end{pmatrix} \quad (9)$$

M is the mass matrix of the system, $\ddot{q}$ is the vector of the system acceleration, Q_e is a vector containing the external forces which are known and λ is a vector containing Lagrange multipliers. The code developed in this work was able to derive automatically the overall matrices M, Q_e, Q_d (the right hand side of the acceleration equation 6), solve equation 9 for $\ddot{\mathbf{q}}$ and λ, and finally integrate the vector for velocity and acceleration to get the system positions and velocities for the next time step.

The system of the motion equations shown in equation 9 does not use explicitly the position and velocity equations associated with the kinematic constraints, that is, equations 1 and 4. This implies that during simulation, chances are that the original constraint equations will be violated. Due to simplicity and easiness of computational implementation, the Baumgarte Stabilization Method (BSM) was employed in this work to control the position and velocity constraint violations brought about by direct integration of equation 9.

The principle behind BSM is to damp out the acceleration constraint violations by feeding back the violations of the position and velocity constraints. Thus, by using the Baumgarte's approach, the equations of motion for a dynamic system subjected to holonomic constraints are represented as,

$$\begin{pmatrix} M & C_q^T \\ C_q & 0 \end{pmatrix} \begin{pmatrix} \ddot{q} \\ \lambda \end{pmatrix} = \begin{pmatrix} Q_e \\ Q_d - 2\alpha\dot{C} - \beta^2 C \end{pmatrix} \quad (10)$$

where α and β are termed as feedback parameters which should be arbitrarily chosen.

In this work, Direct Integration Method (DIM) which involves conversion of the n second-order differential equations of motion into $2n$ first-order differential equations was employed. In DIM, once the second-order differential equations are converted to first-order differential equations, an integration numerical scheme is employed to solve the initial-value problem.

To convert the n second-order differential equations of motion into $2n$ first-order differential equations arrays y and $\dot{y}$ were defined as,

$$y = \begin{pmatrix} q \\ \dot{q} \end{pmatrix}$$
$$\dot{y} = \begin{pmatrix} \dot{q} \\ \ddot{q} \end{pmatrix}$$

The reason for introducing the new vectors y and $\dot{y}$ is that most numerical integration algorithms deal with first-order differential equations. The numerical integration is such that velocities and accelerations at time t, after integration process, yield positions and velocities at next time step, $t = t + \Delta t$.

The computational scheme for the dynamic analysis of mechanical systems which consist of interconnected rigid bodies is as shown in Figure 2.

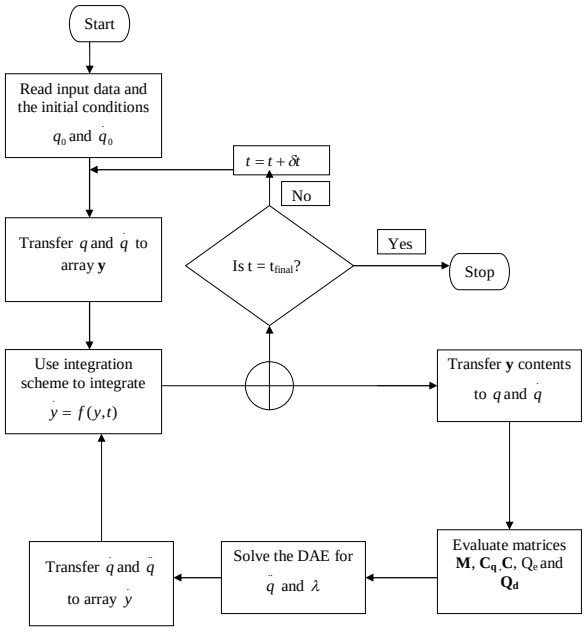

Fig. 2. Flowchart of computational procedure for dynamic analysis of a multi-body system

III. Modeling of Revolute Joints With Clearance

A revolute joint can be described as an assembly of a journal and a bearing in which the journal is free to rotate inside the bearing. In the classical analysis of a revolute joint, the journal and bearing centers are considered always to coincide throughout the motion, that is, the joint is considered ideal or perfect. But in reality, there must be a clearance between the bearing and the journal to permit for the relative motion and the assemblage. The inclusion of the clearance allows for the separation of these centers since the bearing can translate inside the bearing, and hence two degrees of freedom are added to the system by a clearance revolute joint.

A clearance revolute joint does not impose any kinematic constraint on the system since the journal is free to translate inside the bearing. This implies that two kinematic constraints are removed from the system by the revolute clearance joint and two degrees of freedom are added to the system instead. However, the journal is limited to stay inside the bearing walls. In dry contact situations (without lubrication), the journal can move freely within the bearing until contact between the two bodies takes place. When the journal impacts the bearing wall, a normal contact force together with a friction force are evaluated to obtain the dynamics of the real revolute joint. Hence the dynamics of a revolute clearance joint is controlled by the impact-contact forces rather than by the kinematic constraints of the ideal joints.

Since a revolute clearance joint removes two kinematic constraints from the system, the resulting Jacobian Matrix is not square because the total number of coordinate systems will be greater than the total number of the kinematic constraints. For instance, a slider-crank mechanism has four bodies including the ground, each defined with three absolute cartesian coordinates. Hence the total number of coordinates of the mechanism are $4 \times 3 = 12$. When one joint is considered as a clearance joint, then the kinematic constraints are as follows: Constraints due to the fixed link are $1 \times 3 = 3$; constraints due to the two ideal revolute joints are $2 \times 2 = 4$; constraints due to the one ideal prismatic joint are $1 \times 2 = 2$; and one (1) driving constraint. Therefore a slider-crank mechanism with one clearance revolute joint has $3 + 4 + 2 + 1 = 10$ kinematic constraints, implying that the Jacobian Matrix will be a 10×12 matrix. This implies that kinematic analysis cannot be performed on a multi-body system with revolute clearance joint(s), and dynamic analysis will be necessary to solve for the accelerations which can be integrated to get the velocity and position of all bodies and points on the system.

It has been observed that the motion of the journal inside the bearing is in three modes, that is, continuous contact mode, the free-flight mode and the impact mode. In the continuous contact mode, the journal follows the bearing walls and this mode is ended when the journal and bearing separate from each other. In free flight mode, the journal moves freely inside the bearing hence no reaction force is developed at the joint. In the impact mode which occurs at the termination of the free-flight mode, impact forces are applied and removed in the system, and this mode is characterized by discontinuities in the kinematic and dynamic characteristics of the system.

In this work, elements making the clearance revolute joint are modeled as colliding bodies, and the impact between the bodies is treated as a continuous event, that is, the local deformations and the contact forces are continuous functions of time [43]. The impact analysis of the system will be performed by including the contact impact forces during the impact period into the equations of motion as externally applied forces and moments.

A. Kinematic Model of a Revolute Joint with Clearance

In order to simulate a real revolute joint, its necessary to develop a mathematical model for the joint in the multi-body system. Figure 3 shows two bodies *i* and *j* connected with a revolute joint with clearance. Part of body *i* is the bearing while part of body *j* is the journal. X_iY_i and X_jY_j are the body coordinate systems, while XY is the stationary global coordinate system. P_i is the center of the bearing and P_j is the center of the journal at the given instant.

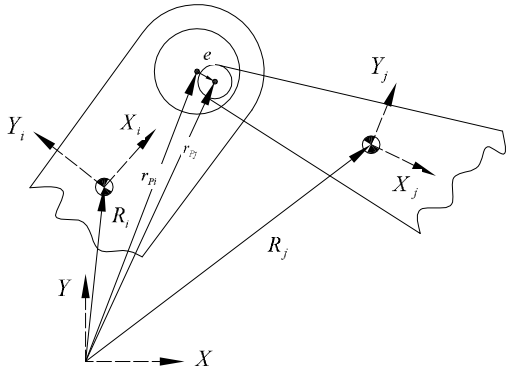

Fig. 3. Generic revolute joint with clearance

The eccentricity vector $\vec{e}$ which connects the centers of the bearing and the journal is given as,

$$\begin{aligned} \vec{e} &= r_{Pj} - r_{Pi} \\ &= \left(R_j + A_j u_{Pj}\right) - \left(R_i + A_i u_{Pi}\right) \end{aligned} \tag{11}$$

where A_i and A_j are the transformation matrices of coordinates X_iY_i and X_jY_j respectively to coordinate XY, and u_{Pi} and u_{Pj} are the coordinates of centers of bodies *i* and *j* with respect to their coordinate systems.

The magnitude of the eccentricity vector is,

$$e = \sqrt{\vec{e}^T \vec{e}} \tag{12}$$

The penetration depth due to the impact between the journal and the bearing can be shown to be,

$$\delta = e - c \tag{13}$$

where c is the radial clearance at the joint which is the difference between the radius of the bearing (R_B) and the radius of the journal (R_J).

The contact points on bodies *i* and *j* during penetration are C_i and C_j respectively as shown in Figure 4.

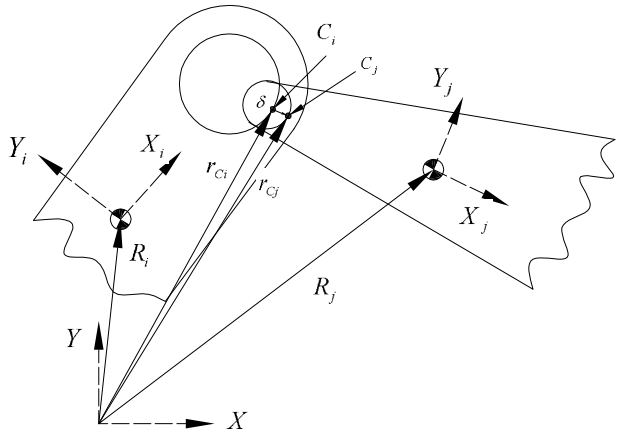

Fig. 4. Penetration depth due to impact between the bearing and the journal

The position of the contact points are given as,

$$r_{Ci} = R_i + A_i u_{Pi} + R_B \vec{n} \quad (14)$$

$$r_{Cj} = R_j + A_j u_{Pj} + R_J \vec{n} \quad (15)$$

where $\vec{n}$ is the unit vector in the direction of penetration caused by the impact between the journal and the bearing, given as,

$$\vec{n} = \frac{\vec{e}}{e} \quad (16)$$

The velocity of the contact points in the global coordinate system is found ny differentiating equations 14 and 15 with respect to time to get,

$$\dot{r}_{Ci} = \dot{R}_i + \dot{A}_i u_{Pi} + R_B \dot{\vec{n}} \quad (17)$$

$$\dot{r}_{Cj} = \dot{R}_j + \dot{A}_j u_{Pj} + R_J \dot{\vec{n}} \quad (18)$$

The components of the relative velocity of the contact points in the normal and tangential plane of collision are represented as $\vec{v}_N$ and $\vec{v}_T$, and are given as,

$$\vec{v}_N = \Big(\dot{r}_{Cj} - \dot{r}_{Ci}\Big)\vec{n} \quad (19)$$

$$\vec{v}_T = \Big(\dot{r}_{Cj} - \dot{r}_{Ci}\Big)\vec{t} \quad (20)$$

where $\vec{t}$ is obtained by rotating $\vec{n}$ anticlockwise by 90^0.

B. Dynamic Model of a Revolute Joint with Clearance

When the journal makes contact with the bearing, then impacts occur and contact-impact forces are created at the joint. Closer inspection of equation 13 shows that;

- When the journal is not in contact with the bearing, $e < c$ and the penetration has a negative value. In this case, the journal is in free-flight motion inside the bearing, and no impact-contact forces are created.
- When contact between the journal and the bearing is established, the penetration has a value equal or greater than zero. In this case, impact-contact forces at the joint are established.

Therefore the computational algorithm developed for dynamic analysis of a system with revolute clearance joint should ensure that impact-contact forces are applied when the depth of penetration is greater or equal to zero.

Since there are velocity components in the normal and tangential directions of the collision between the journal and the bearings as given in equations 19 and 20, then forces are generated in these two directions. The force normal to the direction of collision (F_N) can be evaluated using the contact force laws, such as Hertz, Lankarani-Nikravesh, Dubowsky-Freudenstein or ESDU-78035 contact models, while the force tangential to the direction of collision (F_T) which is the frictional force is evaluated using the appropriate frictional laws.

In this paper, its assumed that no frictional forces are generated during the collision of the bearing and the journal, however friction will be included in further work. Since the direction of the normal unit vector $\vec{n}$ is used as the working direction for the contact forces, then the contact forces at bodies *i* is;

$$F_{Ni} = F_N \vec{n} \quad (21)$$

From the Newton's third law of motion, the contact reaction force at body *j* will be,

$$F_{Nj} = -F_{Ni} \quad (22)$$

These forces which act at the contact points are transferred to the center of masses of bodies *i* and *j* as shown in Figure 5. This transfer of forces from contact forces to the center of masses contributes to the moments given as,

$$M_i = \Big(x_{Ci} - x_i\Big)F_{NiY} - \Big(y_{Ci} - y_i\Big)F_{NiX} \quad (23)$$

$$M_j = \Big(x_{Ci} - x_i\Big)F_{NjY} - \Big(y_{Ci} - y_i\Big)F_{NjX} \quad (24)$$

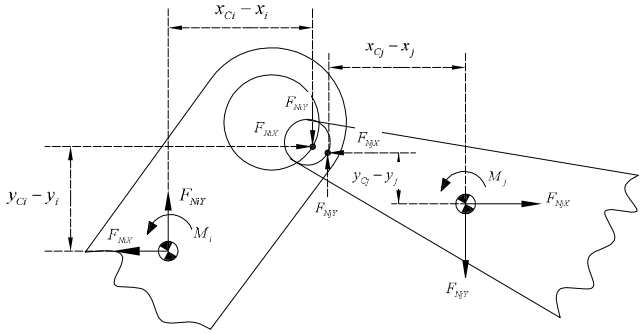

Fig. 5. Transfer of impact forces to the center of masses of the bodies

Once these forces and moments are known and added to the generalized vector of external forces Q_e in equation 10, then the description of the revolute joint with clearance is complete. No kinematic constraint was used when modeling the real joint, instead force constraints have been used.

C. Contact Force Laws

Once the journal makes contact with the bearing, forces normal to the direction of contact are created. In this work

the nonlinear continuous contact force models between two colliding bodies will be used since they represent the physical nature of the contacting surfaces. These contact force modes include; Hertz, Lankarani-Nikravesh, Dubowsky-Freudenstein and ESDU-78035 contact force models.

The Hertz law of contact relates the contact force as a nonlinear power function of the penetration depth as,

$$F_N \;=\; K\delta^n \tag{25}$$

where F_N is the normal contact force, δ is the penetration depth of the contacting bodies given in equation 13, exponent $n = 1.5$ for metallic surfaces and the generalized stiffness K which depends on the material properties and the shape of the contacting surfaces is given as;

$$K \;=\; \frac{4}{3(\sigma_1+\sigma_2)}\Big[\frac{R_1R_2}{R_1+R_2}\Big]^{\frac{1}{2}} \tag{26}$$

where;

R_1 and R_2 are the radii of the spheres (the radius is negative for concave surfaces and positive for convex surfaces)

σ_1 and σ_2 are the material parameters given by;

$$\sigma_i \;=\; \frac{1-\nu_i^2}{E_i} \qquad \text{for } i = 1, 2$$

where E_i and ν_i are the Young's Modulus and Poisson's ratio associated with each sphere.

Unfortunately, the Hertz Law as given in equation 25 does not account for energy dissipation during the impact process and hence cannot be used in both phases of contact (compression and restitution). Lankarani and Nikravesh [44] extended the Hertz contact force model to include a hysteresis damping function to represent the energy dissipated during the impact. The authors separated the normal contact force given in equation 25 into elastic and dissipative components as;

$$F_N \;=\; K\delta^n + D\dot{\delta} \tag{27}$$

where $\dot{\delta}$ is the relative impact velocity given in equation 19, and D is the hysteresis coefficient given as;

$$D \;=\; \Big[\frac{3K(1-c_e^2)}{4\dot{\delta}^{(-)}}\Big]\delta^n \tag{28}$$

where $\dot{\delta}^{(-)}$ is the initial impact velocity. Therefore the final normal contact force can be expressed as;

$$F_N \;=\; K\delta^n\Big[1+\frac{3(1-c_e^2)\dot{\delta}}{4\dot{\delta}^{(-)}}\Big] \tag{29}$$

Equation 29 is only valid for impact velocities lower than the propagation velocity of elastic waves across the bodies, i.e., $\dot{\delta} \leq 10^{-5}\sqrt{\frac{E}{\rho}}$ where E is the Young's modulus and ρ is the material mass density [45].

The contact models given by equations 25 and 29 are applicable for colliding bodies with spherical contact areas. Various elastic models have been put forward for the cylindrical contact surfaces, with the commonly used ones being the Dubowsky and Fruedenstein model and the ESDU-78035 model, both of which are given as equations 30 and 31 respectively;

$$\delta \;=\; F_N\Big(\frac{\sigma_1+\sigma_2}{L}\Big)\Big[\ln\Big(\frac{L^3(R_1-R_2)}{F_NR_1R_2(\sigma_1-\sigma_2)}\Big)+1\Big] \tag{30}$$

and

$$\delta \;=\; F_N\Big(\frac{\sigma_1+\sigma_2}{L}\Big)\Big[\ln\Big(\frac{4L(R_1-R_2)}{F_N(\sigma_1+\sigma_2)}\Big)+1\Big] \tag{31}$$

where L is the length of the cylinder. Equations 30 and 31 are nonlinear function for F_N and require an iterative scheme, such as Newton-Raphson method to solve for the normal contact force F_N for a known penetration depth δ. Also, these models do not account for energy dissipation during the impact process.

IV. Results and Discussions

This section contains extensive results obtained from computational simulations of a slider-crank mechanism with a revolute clearance joint. Two major cases are considered, that is;

(a) Case 1: When revolute clearance joint only exist between the crank and the connecting rod.
(b) Case 2: When revolute clearance joint only exist between the connecting rod and the slider.

This study takes into account three main functional parameters of the slider-crank mechanism, that is, the location of the considered clearance joint, clearance size and the input crank speed.

A. Description of the Slider-Crank Mechanism

A typical slider-crank mechanism as shown in Figure 6 is used as a demonstrative example to study the parametric effect of revolute joint clearance on the dynamic response of a multibody mechanical system.

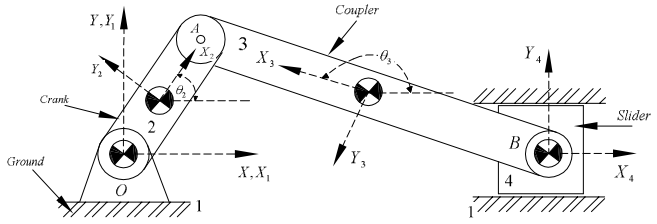

Fig. 6.

The slider-crank mechanism considered has the following parameters: Length of crank $L_{OA} = 0.05m$, length of the coupler link $L_{AB} = 0.12m$, mass of the crank $m_2 = 0.3kg$, mass of the coupler $m_3 = 0.21kg$, mass of the slider $m_4 = 0.14kg$, moment of inertia of crank about its center of gravity, $I_2 = 0.00001kg.m^2$ and moment of inertia of coupler about its center of gravity, $I_2 = 0.00025kg.m^2$. In addition all the links are assumed to be uniform such that their centers of gravity are at their geometric centers. The following are other parameters used for the different contact models: Nominal bearing diameter d=10mm, Length of the cylindrical contact between the journal and the bearing L=20mm, Coefficient of

restitution C_e=0.9, Young's modulus E=207MPa, Poisson's ratio ν=0.3 and integration time step Δt=0.000001s

In the simulations, the initial configuration of the mechanism is defined when the crank and the connecting rod are collinear, and the journal and the bearing centers of the considered clearance revolute joint to coincide. The initial positions and velocities necessary to start the dynamic simulation are obtained from kinematic simulation of the slider-crank mechanism in which all the joints are considered perfect.

The dynamic response of the slider-crank mechanism is presented by plotting the variations with time of the slider velocity, slider acceleration, reaction force at the clearance joint and torque required to maintain constant speed of the crank. The results are presented for four cycles of the mechanism after the first cycle when steady state is reached. The first cycle has instability due to the fact that the mechanism is moved from rest and because of the inertia, great impact occurs between the journal and the bearing of the revolute joint at the start of the simulation. The behavior of the revolute clearance joints is also illustrated by using the slider velocity and the slider acceleration to plot the Poincaré maps at different test scenarios.

B. Results for Different Contact Force Models

In this subsection, the dynamic responses of the slider-crank mechanism when joint A is separately modeled with 0.3mm clearance, and also when joint B is separately modeled with 0.3mm clearance using the four commonly known nonlinear contact laws.

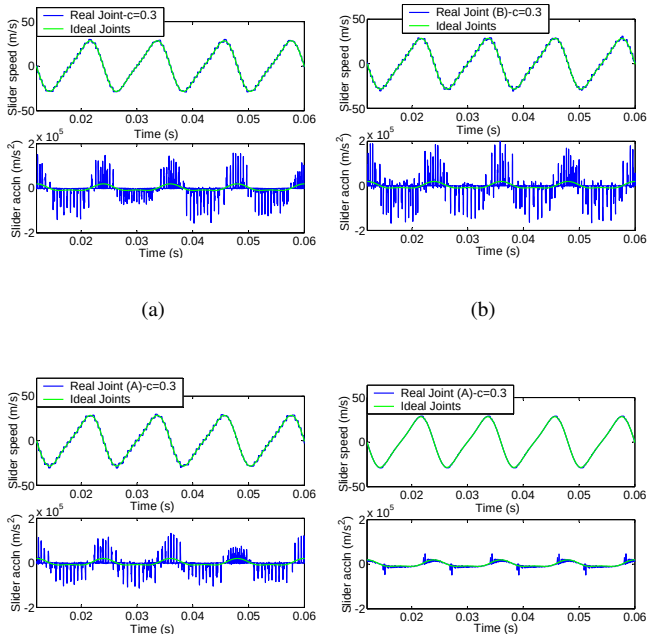

Fig. 7. Slider linear velocity and acceleration responses when revolute joint A is modeled with a 0.3mm clearance using (a) Hertz contact force law (b) Dubowsky-Freudensteins contact force law (c) ESDU-78035 contact force law and (d) Lankarani-Nikravesh contact force law

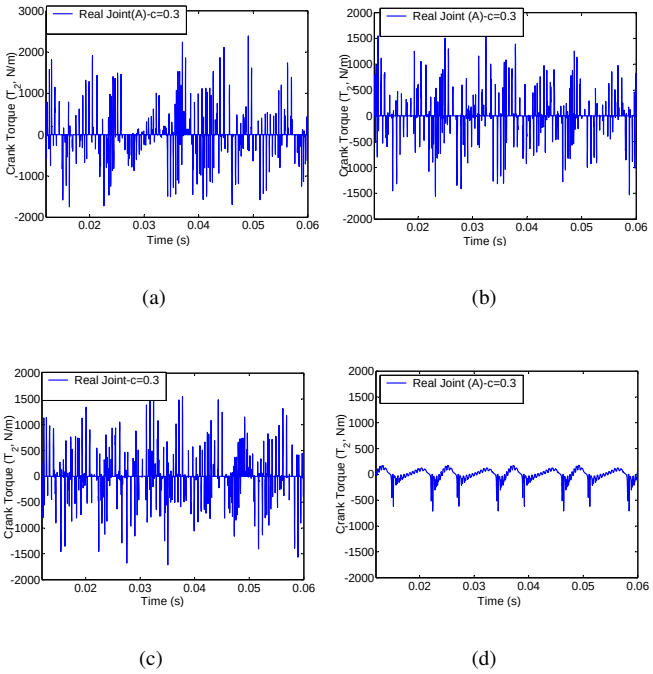

Fig. 8. Driving torque responses when revolute joint A is modeled with a 0.3mm clearance using (a) Hertz contact force law (b) Dubowsky-Freudensteins contact force law (c) ESDU-78035 contact force law and (d) Lankarani-Nikravesh contact force law

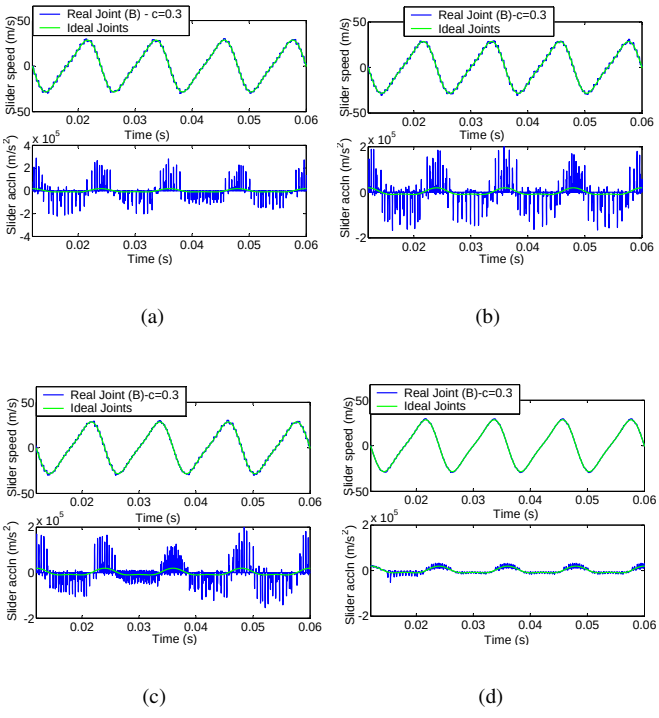

Fig. 9. Slider linear velocity and acceleration responses when revolute joint B is modeled with a 0.3mm clearance using (a) Hertz contact force law (b) Dubowsky-Freudensteins contact force law (c) ESDU-78035 contact force law and (d) Lankarani-Nikravesh contact force law

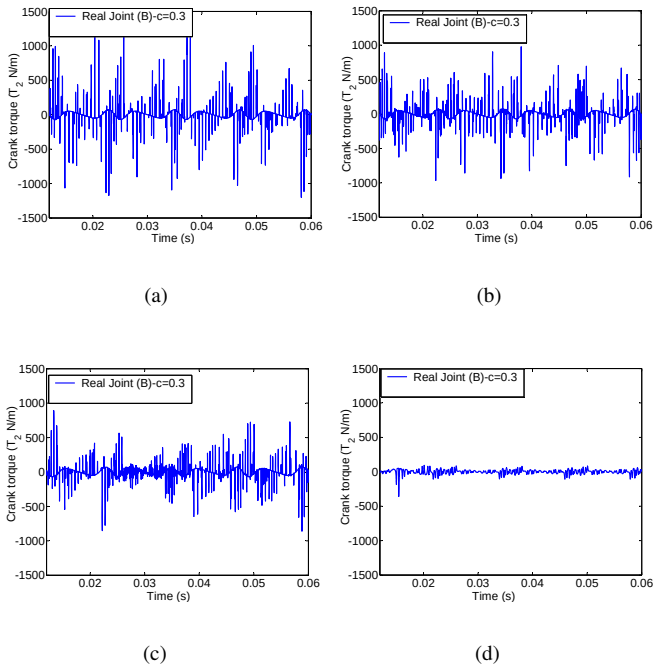

Fig. 10. Driving torque responses when revolute joint B is modeled with a 0.3mm clearance using (a) Hertz contact force law (b) Dubowsky-Freudensteins contact force law (c) ESDU-78035 contact force law and (d) Lankarani-Nikravesh contact force law

The influence of the joint clearance is clearly observed at the stair-case shaped velocity curves. The horizontal lines in the velocity curves indicate that the journal is in free-flight motion inside the bearing, and the slider moves with a constant velocity. Sudden changes in velocity of the slider is due to impacts between the journal and the bearing. These impacts are also visible in the acceleration curves by high peak values. Also smooth changes in velocity are observed implying that the journal and the bearing are in continuous contact motion, that is, the journal follows the bearing wall. This situation is confirmed by the smooth changes in the acceleration curve.

The elastic contact models, that is, Hertz, Dubowsky-Freudensteins and ESDU-78035 contact models, which do not account for energy dissipation lead to high peaks for the slider acceleration and the torque required to drive the crank with a constant angular velocity. The continuous contact force model proposed by Lankarani and Nikravesh presents much lower slider acceleration and crank torque peaks, due to the dissipative energy features of the model. Such energy dissipation is also reflected at the slider velocity and acceleration curves by the long periods of time for which the journal and bearing are in continuous contact mode. There is no much difference between the three nonlinear elastic contact laws. This implies that the two cylindrical contact models (that is, Dubowsky-Freudensteins and ESDU-78035 contact models) do not present any advantage compared to the elastic spherical contact model (that is, the Hertz contact model). However, the cylindrical models are nonlinear and implicit functions, and therefore they require an iterative procedure such as Newton-Raphson algorithm to solve them which is computationally time consuming. The Hertz relation along with the modification to include the energy dissipation in the form of internal damping (that is, the Lankarani-Nikravesh model) has been adopted by many researchers and has proven to produce results which correlate well with the experimental ones. Therefore, in the preceding results, the model proposed by Lankarani and Nikravesh will be employed when modeling the contact-impact forces in a revolute clearance joint.

It is also observed that the slider acceleration peaks when Joint B is modeled as a real joint are higher than the acceleration peaks produced when Joint A is modeled as a real joint. In addition, the crank torques obtained when Joint A is modeled as a real joint have higher peaks as compared to the peaks of crank torques obtained when Joint B is modeled as a real joint. An explanation to these observations will be sought and made once such behaviors are validated experimentally.

C. Influence of the Clearance Size

In this subsection, the influence of the clearance size at Joint A and also at Joint B on the dynamic behavior of the slider-crank mechanism is investigated and comparisons presented. The range of the clearances used at each joint is 0.01mm, 0.1mm, 0.3mm and 0.5mm, and the crank rotates uniformly at 5000rev/min. Figures 11(a) to 14(d) show the results when only Joint A is modeled as a clearance revolute joint, while Figures 15(a) to 18(d) present the results when only Joint B is modeled as a clearance revolute joint. The results presented are the time plots of the slider acceleration, the reaction force produced in the clearance joint, the reaction moment that acts on the crank and the Poincaré map.

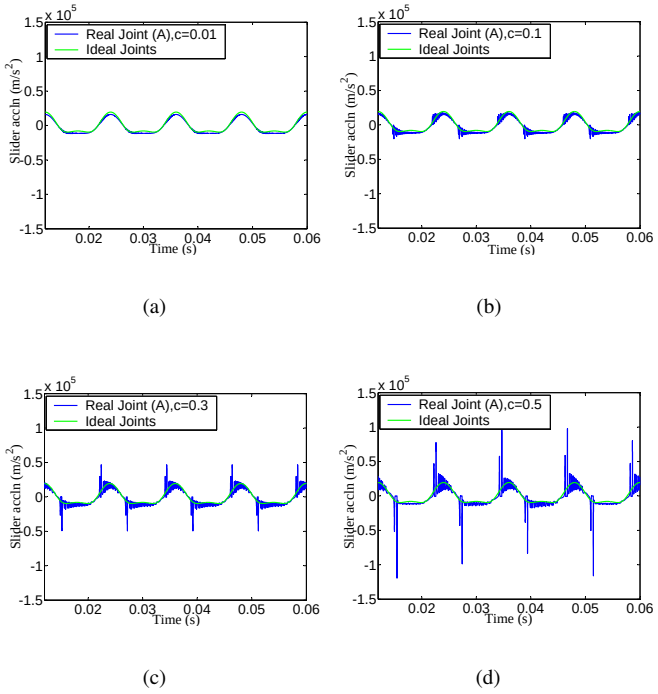

Fig. 11. Slider acceleration responses for different clearance sizes at joint A (a) 0.01mm (b) 0.1mm (c) 0.3mm (d) 0.5mm

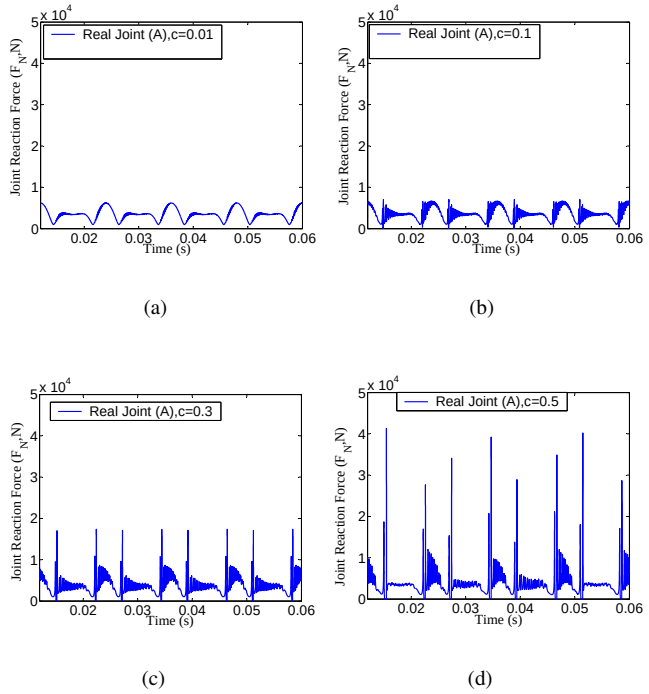

Fig. 12. Joint reaction force responses for different clearance sizes at joint A (a) 0.01mm (b) 0.1mm (c) 0.3mm (d) 0.5mm

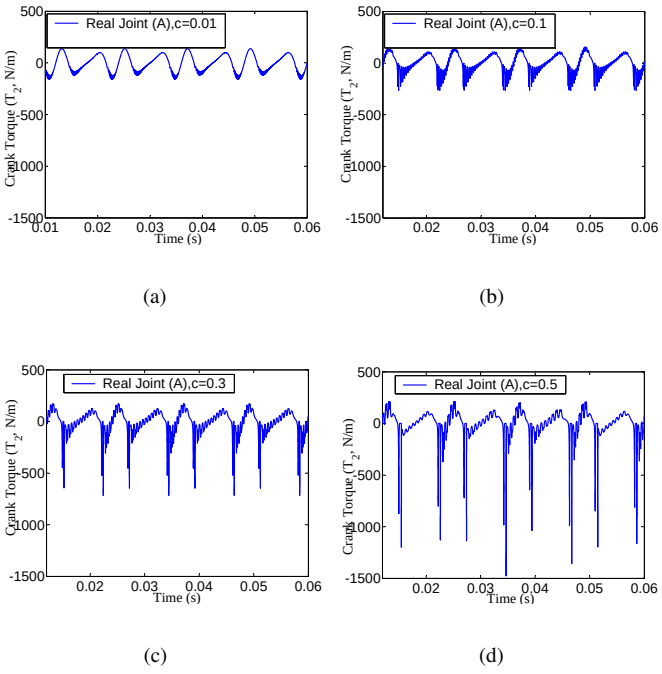

Fig. 13. Crank torque responses for different clearance sizes at joint A (a) 0.01mm (b) 0.1mm (c) 0.3mm (d) 0.5mm

Figures 11(a) to 13(d) show that increasing the clearance size of a revolute joint A, the mechanism experiences increased peaks of the slider acceleration, joint reaction force and the crank moment. This implies that at higher joint clearances,

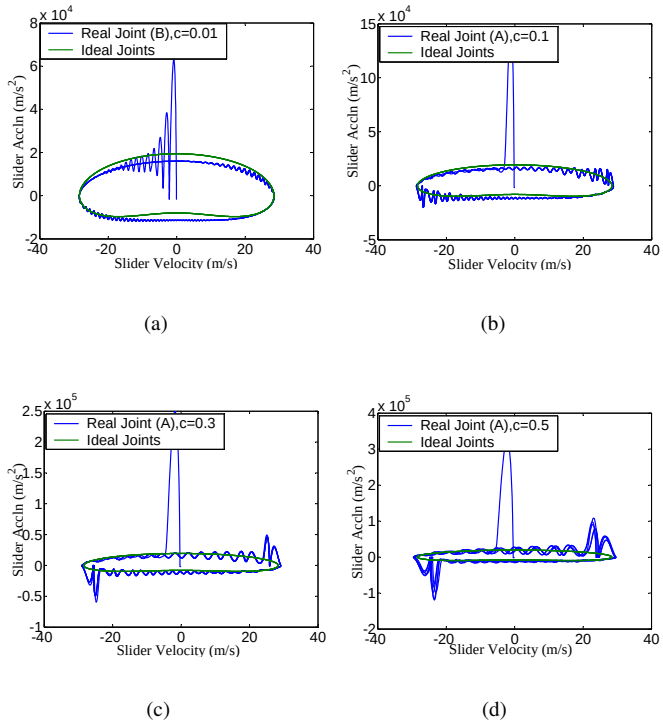

Fig. 14. Poincaré maps for different clearance sizes at joint A (a) 0.01mm (b) 0.1mm (c) 0.3mm (d) 0.5mm

higher impacts followed by rebounds take place, instead of continuous or permanent contact between the journal and the bearing walls. When the clearance is small, the system response tends to be closer to the ideal response as evident in Figures 11(a), 12(a) and 13(a). This implies that at smaller clearance, the journal and the bearing of the joint experience a smaller number of impacts and the journal follows the bearing wall. This is also evident in the the Poincaré maps presented in Figures 14(a) to 14(d), from which it is clearly observed that increasing the radial clearance of the joint from 0.01mm to 0.5mm, the behavior of the system changes from periodic to quasi-periodic. This quasi-periodic behavior is evident in the map because at large clearance sizes (0.3mm and 0.5mm), cycles of the mechanism fill up the map in a fully predictable manner. When the clearance is small (0.01mm and 0.1mm), the behavior of the system tends to be periodic since the cycles of the mechanism follow the same path in the map. However, increasing the clearance size beyond 0.5mm the behavior of the system changed from quasi-periodic to chaotic. Also at large clearance sizes such as 0.3mm and 0.5mm, the three types of journal motion inside the bearing are observed, namely, the free-flight motion, the impact mode and the permanent or continuous contact mode.

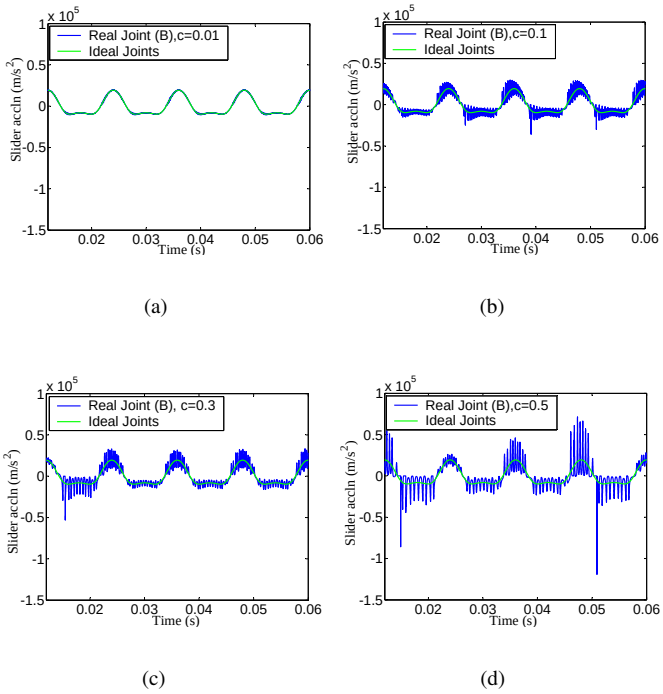

Fig. 15. Slider acceleration responses for different clearance sizes at joint B (a) 0.01mm (b) 0.1mm (c) 0.3mm (d) 0.5mm

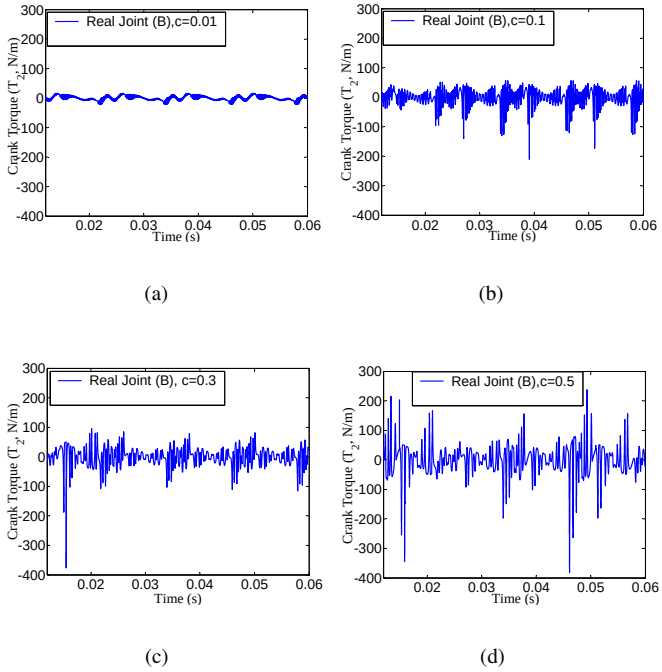

Fig. 17. Crank torque responses for different clearance sizes at joint B (a) 0.01mm (b) 0.1mm (c) 0.3mm (d) 0.5mm

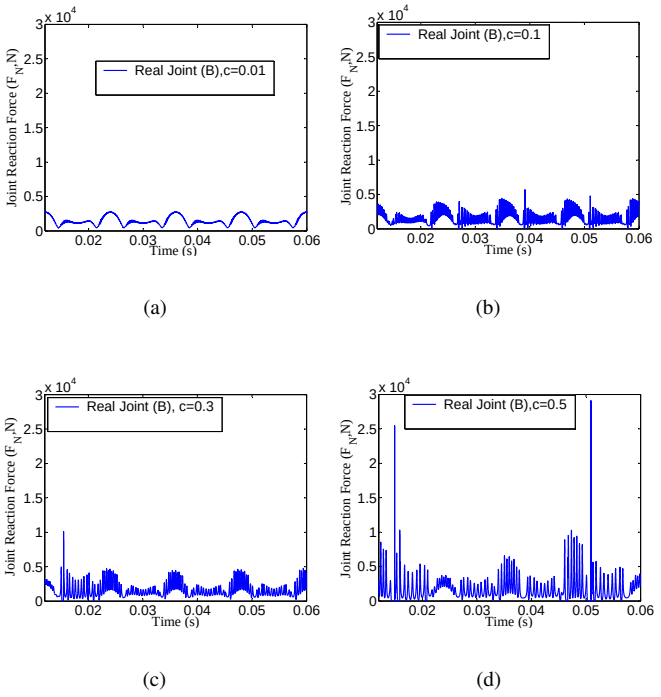

Fig. 16. Joint reaction force responses for different clearance sizes at joint B (a) 0.01mm (b) 0.1mm (c) 0.3mm (d) 0.5mm

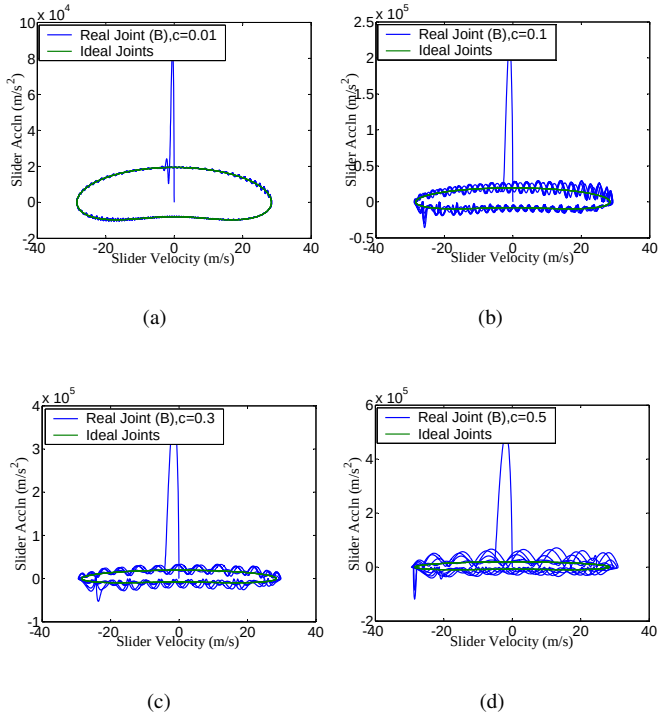

Fig. 18. Poincaré maps for different clearance sizes at joint B (a) 0.01mm (b) 0.1mm (c) 0.3mm (d) 0.5mm

From Figures 15(a) to 17(d), its also seen that increasing the clearance size of the revolute joint B, the mechanism experiences increased peaks of the slider acceleration, joint reaction force and the crank moment. However, as seen in Figures 18(a) to 18(d), increasing the radial clearance of the joint from 0.01mm to 0.5mm, the behavior of the system

changes from periodic to quasi-periodic, and then to chaotic. The chaotic behavior is evident in Fig. 18(d) since at a joint clearance of 0.5mm, different cycles of the mechanism lead to different curves in the map in an unpredictable manner. This behavior is different from the one witnessed when only Joint A was modeled as a revolute clearance joint, in which at a clearance of 0.5mm the behavior of the system was still quasi-periodic. This shows that the dynamics of the revolute clearance Joint B in the slider-crank mechanism is more sensitive to the clearance size as compared to that of revolute clearance Joint A. This confirms the already made observation that, dynamic response peaks of the mechanism when Joint B is modeled as a real joint are higher than the peaks produced when Joint A is modeled as a real joint with the same radial clearances. Although, the clearances of different joints in a system show almost the same effects on the dynamic response of the system, it has been shown that the joints will have different sensitivities to the clearance size. Therefore in order to design effective controllers for eliminating fully the chaotic behaviors brought about by the non-linearities of joints with clearances, the dynamic effect of each joint on the system should be understood, that is, the effects of clearance sizes in one joint cannot be used as a general case in a mechanical system.

D. Influence of the Input Crank Velocity

The range of the input crank speeds used at each joint is 800rpm, 1200rpm, 2500rpm and 5000rpm, and the radial clearance at each joint is 0.3mm. Figures 19(a) to 22(d) show the results when only Joint A is modeled as a clearance revolute joint, while Figures 23(a) to 26(d) present the results when only Joint B is modeled as a clearance revolute joint.

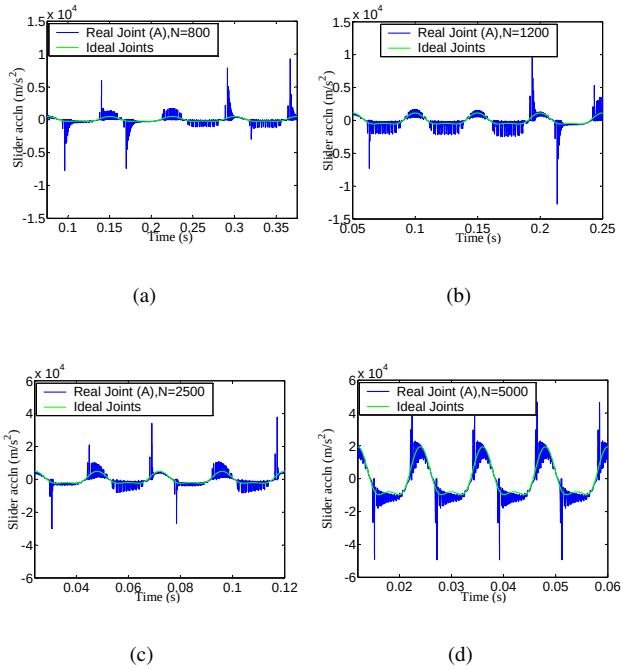

Fig. 19. Slider acceleration responses for 0.3mm clearance size at joint A for different crank speeds (a) 800rpm (b) 1200rpm (c) 2500rpm (d) 5000rpm

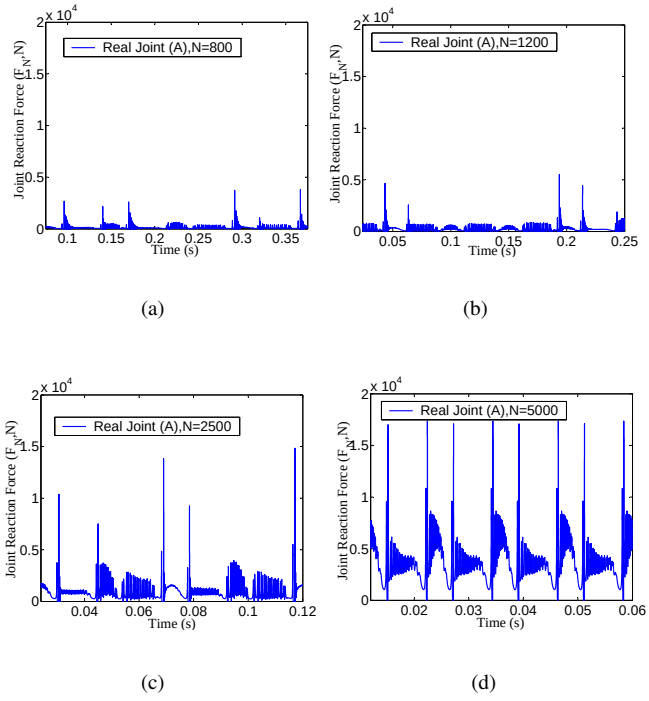

Fig. 20. Joint reaction force responses for 0.3mm clearance size at joint A for different crank speeds (a) 800rpm (b) 1200rpm (c) 2500rpm (d) 5000rpm

Figures 19(a) to 21(d) show that increasing the rotational speed of the crank, the mechanism experiences increased peaks of the slider acceleration, joint reaction force and the crank moment due to collisions between the journal and the bearing

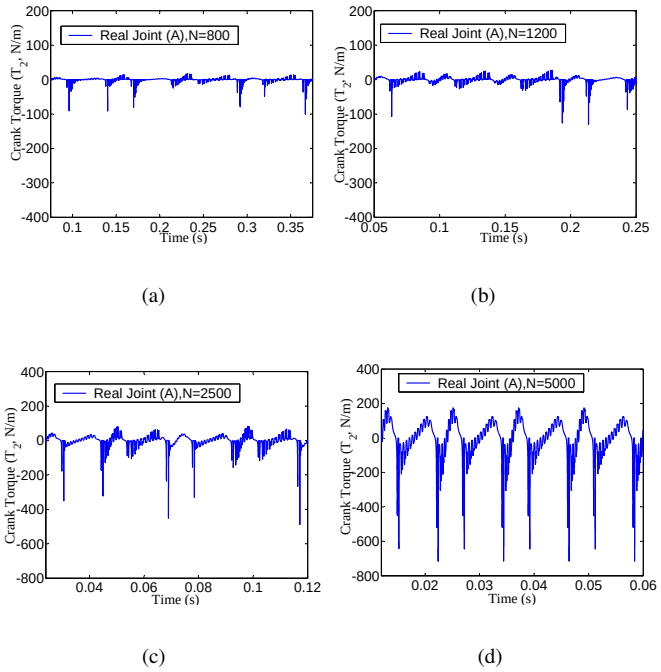

Fig. 21. Crank torque responses for 0.3mm clearance size at joint A for different crank speeds (a) 800rpm (b) 1200rpm (c) 2500rpm (d) 5000rpm

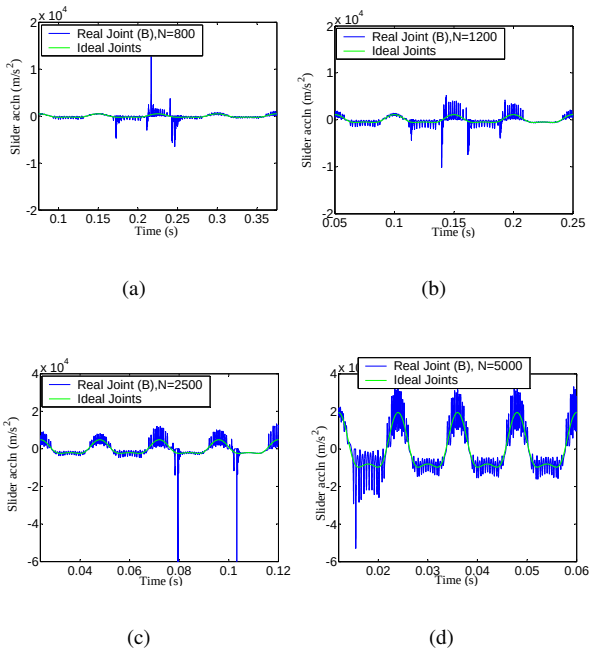

Fig. 23. Slider acceleration responses for 0.3mm clearance size at joint B for different crank speeds (a) 800rpm (b) 1200rpm (c) 2500rpm (d) 5000rpm

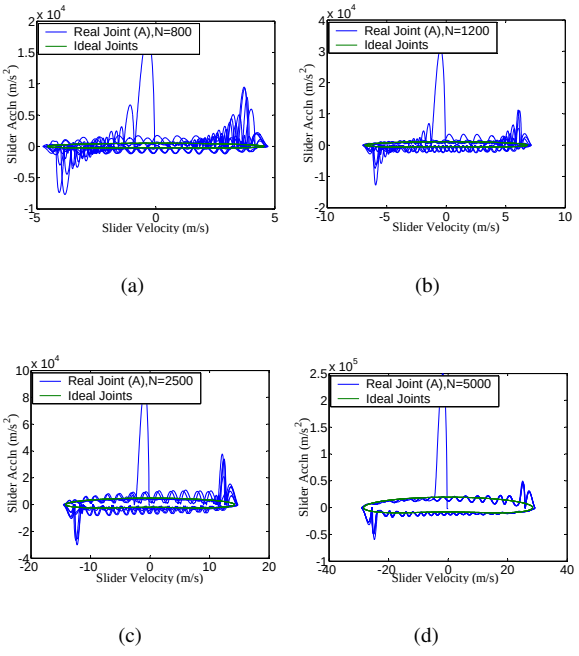

Fig. 22. Poincaré maps for 0.3mm clearance size at joint A for different crank speeds (a) 800rpm (b) 1200rpm (c) 2500rpm (d) 5000rpm

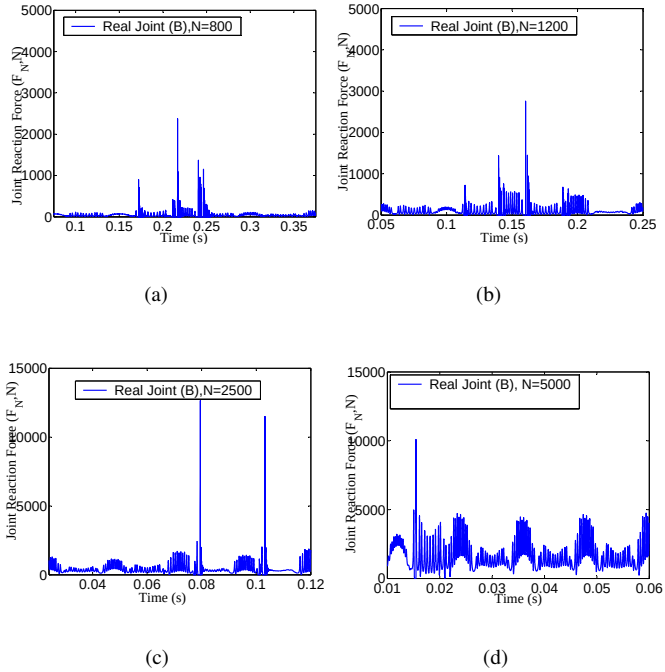

Fig. 24. Joint reaction force responses for 0.3mm clearance size at joint B for different crank speeds (a) 800rpm (b) 1200rpm (c) 2500rpm (d) 5000rpm

of the clearance Joint A. However the Poincaré maps presented in Figures 22(a) to 22(d) show that when the crank speed is increased from 800rpm to 5000rpm while holding the radial clearance of Joint A constant, the behavior of the system changes from chaotic to quasi-periodic, and then to periodic at a speed of 5000rpm.

Figures 23(a) to 25(d) show that increasing the rotational speed of the crank, the mechanism experiences increased peaks of the slider acceleration, joint reaction force and the crank moment due to collisions between the journal and the bearing of the clearance Joint B. However the Poincaré maps presented

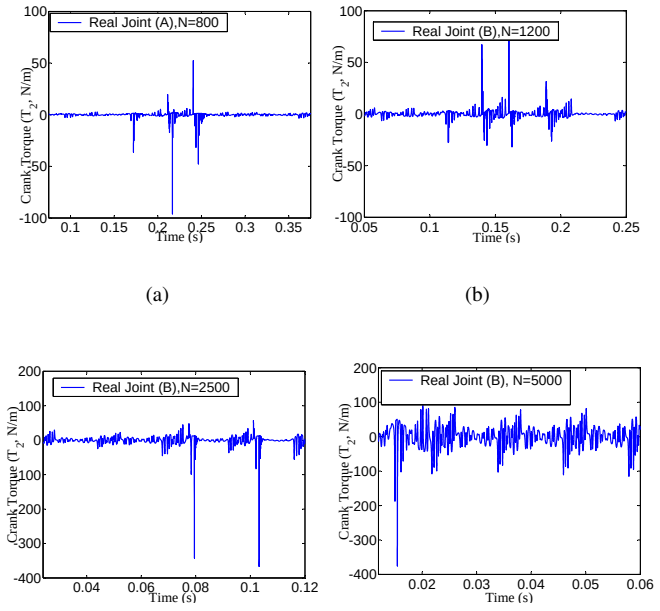

Fig. 25. Crank torque responses for 0.3mm clearance size at joint B for different crank speeds (a) 800rpm (b) 1200rpm (c) 2500rpm (d) 5000rpm

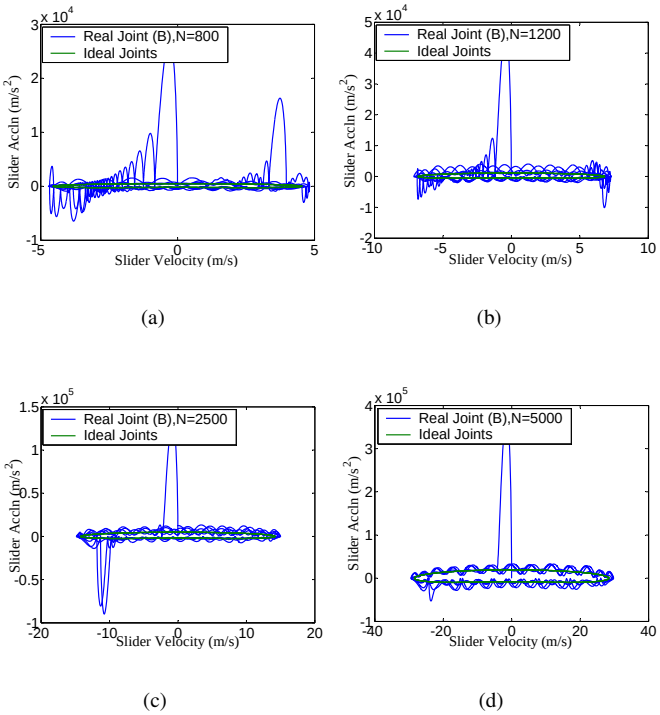

Fig. 26. Poincaré maps for 0.3mm clearance size at joint B for different crank speeds (a) 800rpm (b) 1200rpm (c) 2500rpm (d) 5000rpm

in Figures 26(a) to 26(d) show that when the crank speed is increased from 800rpm to 5000rpm while holding the radial clearance of Joint B constant, the behavior of the system changes from periodic to quasi-periodic and then to chaotic at a speed of 5000rpm. This behavior is different from the one witnessed when only Joint A was modeled as a revolute clearance joint, in which the behavior changes from chaotic to periodic when the speed of the crank is increased as shown in Figures 22(a) to 22(d). Although, the crank speed variations in the mechanism show almost the same effects on the dynamic response of the system with differently positioned clearance joints, a closer analysis shows that increasing the driving speed of a mechanism, the behavior of the mechanism may change from either periodic to chaotic, or chaotic to periodic depending on which joint has clearance. Therefore in order to design effective controllers for eliminating fully the chaotic behaviors brought about by the non-linearities of joints with clearances, the dynamic effect of each joint on the system should be understood, that is, the effects of driving speeds in one clearance joint cannot be used as a general case in a mechanical system.

V. Conclusion

From the numerical simulations presented in this work, it can be concluded that the dynamic response of a multi-body mechanical system with revolute clearance joint depends on the location of the joint, the clearance size and the operating speed of the system. It is clear that the dynamics of the revolute clearance joint in a mechanical system is quite sensitive to the clearance size such that by slightly changing the value of the clearance size, the response of the system can shift from chaotic to periodic behavior and vice-versa. However, the degree of sensitivity to the clearance size varies from one joint to another. For instance in a slider-crank mechanism, the joint between the slider and connecting rod is more sensitive to the clearance size than the joint between the crank and the connecting rod. This explains why many researchers have emphasized on modeling the joint between the slider and connecting rod as a clearance joint.

Other than the clearance size, the operating speed of the multi-body mechanical system has been observed to affect significantly the dynamic response of a system with revolute clearance joint. The higher the operating speed, the higher the impact forces at the clearance joint. However, increasing the driving speed of a multi-body mechanical, the behavior of the mechanism may change from either periodic to chaotic, or chaotic to periodic depending on which joint has clearance. Therefore in order to design effective controllers for eliminating fully the chaotic behaviors brought about by the non-linearities of joints with clearances, the dynamic effect of each joint on the system should be understood. This is because the effects of the clearance sizes and driving speeds in one clearance joint cannot be used as a general case in a mechanical system.

Acknowledgment

The authors gratefully acknowledge the financial and logistical support of Jomo Kenyatta University of Agriculture and Technology (JKUAT) and the German Academic Exchange Service (DAAD) on the ongoing PhD research project titled

'Dynamic Analysis of Flexible Multi-Body Mechanical Systems with Imperfect Kinematic Joints'.

The advice of Prof. Parviz Nikravesh of University of Arizona during the development of the MATLAB code for kinematic and dynamic analysis of a general planar multi-body mechanical system is highly appreciated.

REFERENCES

[1] Dubowsky, S. and Freudenstein, F., "Dynamic analysis of mechanical systems with clearances, part 1: Formulation of dynamic model," *Journal of Engineering for Industry*, vol. 93(1), pp. 305–309, 1971.

[2] Dubowsky, S. and Freudenstein, F., "Dynamic analysis of mechanical systems with clearances, part 2: Dynamic response," *Journal of Engineering for Industry,*, vol. 93(1), pp. 310–316, 1971.

[3] Dubowsky, S., Deck, J. F. and Costello, H., "The dynamic modeling of flexible spatial machine systems with clearance connections," *Journal of Mechanisms, Transmissions and Automation in Design*, vol. 109, pp. 87–94, 1987.

[4] Earles, S.W.E. and Wu, C.L.S., "Motion analysis of a rigid link mechanism with clearance at a bearing using lagrangian mechanics and digital computation," *Journal of Mechanisms*, pp. 83–89, 1973.

[5] Wu, C.L.S. and Earles, S.W.E., "A determination of contact-loss at a bearing of a linkage mechanism," *Journal of Engineering for Industry*, vol. 99(2), pp. 375–380, 1977.

[6] Furuhashi, T., Morita, N. and Matsuura, M., "Research on dynamics of four-bar linkage with clearances at turning pairs 1st report: General theory using continuous contact model," *JSME*, vol. 21, pp. 518–523, 1978.

[7] Furuhashi, T., Morita, N. and Matsuura, M., "Research on dynamics of four-bar linkage with clearances at turning pairs 2nd report: Analysis of crank-lever mechanism with clearance at joint of crank coupler using continuous contact model," *JSME*, vol. 21, pp. 1284–1291, 1978.

[8] Furuhashi, T., Morita, N. and Matsuura, M., "Research on dynamics of four-bar linkage with clearances at turning pairs 3rd report: Analysis of crank-lever mechanism with clearance at joint of coupler and lever using continuous contact model," *JSME*, vol. 21, pp. 1292–1298, 1978.

[9] Furuhashi, T., Morita, N. and Matsuura, M., "Research on dynamics of four-bar linkage with clearances at turning pairs 4th report: Forces acting at joints of crank-lever mechanism," *JSME*, vol. 21, pp. 1292–1298, 1978.

[10] Farahanchi, F. and Shaw, S. W., "Chaotic and periodic dynamics of a slider-crank mechanism with slider clearance," *Journal of Sound and Vibration*, vol. 177(3), pp. 307–324, 1994.

[11] Rhee, J. and Akay A., "Dynamic response of a revolute joint with clearance," *Journal of Mechanisms and Machine Theory*, vol. 31(1), pp. 121–134., 1996.

[12] Ravn, P., "A continuous analysis method for planar multibody systems with joint clearance," *Journal of Multibody System Dynamics*, vol. 2, pp. 1–24, 1998.

[13] Ravn, P., Shivaswamy, S., Alshaer, B. J. and Lankarani, H. M., "Joint clearances with lubricated long bearings in multibody mechanical systems," *Journal of Mechanical Design*, vol. 122, pp. 484–488, 2000.

[14] Chunmei, J., Yang, Q., Ling, F. and Ling, Z., "The nonlinear dynamic behavior of an elastic linkage mechanism with clearances," *Journal of Sound and Vibration*, vol. 249(2), pp. 213–226, 2002.

[15] Chang, Z., "Nonlinear dynamics and analysis of four-bar linkage with clearance," in *In Proceedings of 12th IFToMM Congress, France*, 2007.

[16] Schwab, A.L., Meijaard, J.P. and Meijers, P. , "A comparison of revolute joint clearance models in the dynamic analysis of rigid and elastic mechanical systems," vol. 37, pp. 895–913, 2002.

[17] Flores, P., Ambrosio, J., Claro, J.P., "Dynamic analysis for planar multibody mechanical systems with lubricated joints," *Journal of Multibody Systems Dynamics*, vol. 12, pp. 47–74, 2004.

[18] Flores, P., and Ambrosio, J., "Revolute joints with clearance in multibody systems," *Journal of Computers and Structures*, vol. 82, pp. 1359–1369, 2004.

[19] Erkaya, S., and Uzmay, I., "Experimental investigation of joint clearance effects on the dynamics of a slider-crank mechanism," *Journal of Multibody System Dynamics*, vol. 24, pp. 81–102, 2010.

[20] Shiau, T.N., Tsai, Y.J., Tsai, M.S., "Nonlinear dynamic analysis of a parallel mechanism with consideration of joint effects," *Journal of Mechanism and Machine Theory*, vol. 43, pp. 491–505, 2008.

[21] Erkaya, S. and Uzmay, I., "A neural-genetic (nn-ga) approach for optimising mechanisms having joints with clearance," *Journal of Multibody Systems Dynamics*, vol. 20, pp. 69–83, 2008.

[22] Erkaya, S., and Uzmay, I., "Determining link parameters using genetic algorithm in mechanisms with joint clearance," *Journal of Mechanisms and Machine Theory*, vol. 44, pp. 222–234, 2009.

[23] Erkaya, S., and Uzmay, I., "Optimization of transmission angle for slider-crank mechanism with joint clearances," *Journal of Structural Multidiscipine Optimization*, vol. 37, pp. 493–508, 2009.

[24] Khemili, I., and Romdhane, L., "Dynamic analysis of a flexible slider-crank mechanism with clearance," *European Journal of Mechanics, Elsevier*, vol. 27, pp. 882–898, 2008.

[25] Erkaya, S., and Uzmay, I., "Investigation on effect of joint clearance on dynamics of four-bar mechanism," *Journal of Nonlinear Dynamics*, vol. 58, pp. 179–198, 2009.

[26] Liu, T. S. and Lin, Y. S., "Dynamic analysis of flexible linkages with lubricated joints," *Journal of Sound and Vibration*, vol. 141, pp. 193–205, 1990.

[27] Ravn, P., Shivaswamy, S. and Lankarani, H. M., "Treatment of lubrication in long bearings for joint clearances in multibody mechanical systems," in *Proceedings of the ASME Design Technical Conference*, Las Vegas, September 12-15 1999.

[28] Olivier, A. B. and Rodriguez, J., "Modeling of Joints with Clearance in Flexible Multibody Systems," *International Journal of Solids and Structures*, vol. 39, pp. 41–63, 2002.

[29] Kakizaki, T., Deck, J.F. and Dubowsky, S., "Modeling the spatial dynamics of robotic manipulators with flexible links and joint clearances," *Journal of Mechanical Design*, vol. 115, pp. 839–847, 1993.

[30] Jia, X., Jin, D., Ji, L., and Zhang, J., "Investigation on the dynamic performance of the tripod-ball sliding joint with clearance in a crank-slider mechanism. part 1. theoretical and experimental results.," *Journal of Sound and Vibrations*, vol. 252(5), p. 919933, 2002.

[31] Bing, S. and Ye, J., "Dynamic analysis of the reheat-stop-valve mechanism with revolute clearance joint in consideration of thermal effect.," *Journal of Mechanisms and Machine Theory*, vol. 43(12), pp. 1625–1638, 2008.

[32] Flores, P., "Modeling and simulation of wear in revolute clearance joints in multibody systems," *Journal of Mechanisms and machine Theory*, vol. 44(6), pp. 1211–1222, 2009.

[33] Dupac, M. and Beale, D.G., "Dynamic analysis of a flexible linkage mechanism with cracks and clearance." To be published in Journal of Mechanisms and Machine Theory, 2010.

[34] Flores, P., Ambrsio, J., Claro, J.C.P., Lankarani, H.M. and Koshy, C.S., "Lubricated revolute joints in rigid multibody systems," *Journal of Nonlinear Dynamics*, vol. 56(3), pp. 277–295, 2009.

[35] Mukras, S., Kim, N.H., Mauntler, N.A., Schmitz, T.L., and Sawyer, W.G., "Analysis of planar multibody systems with revolute joint wear," *Journal of Wear*, vol. 268, pp. 643–652, 2010.

[36] Flores, P., "A parametric study on the dynamic response of plnar multibody systems with multiple clearance joints," *Journal of Nonlinear Dynamics*, vol. 4, pp. 633–653, 2010.

[37] Dubowsky, S., and Moening, M.F., "An Experimental and Analytical Study of Impact Forces in Elastic Mechanical Systems with Clearances," *Journal of Mechanism and Machine Theory*, vol. 13, pp. 451–465, 1978.

[38] Flores, P., *Dynamic Analysis of Mechanical Systems with Imperfect Kinematic Joints*. PhD thesis, UNIVERSIDADE DO MINHO PARA, 2004.

[39] Cheriyan, S. K., *Chracterization of Mechanical Systems with Real Joints and Flexible Links*. PhD thesis, Wichita State University, 2006.

[40] Nikravesh, P.E., *Computer-Aided Analysis of Mechanical Systems,*. Prentice Hall, Englewood Cliffs, New Jersey, 1988.

[41] Baumgarte, J., "Stabilization of constraints and integrals of motion in dynamical systems," *Journal of Computer Methods in Applied Mechanics and Engineering*, vol. 1, pp. 1–16, 1972.

[42] Shabana, A. A., *Computational Dynamics*. John Wiley & Sons, New York, 1994.

[43] Lankarani, H. M. and Nikravesh, P. E., "Continuous contact force models for impact analysis in multibody systems," *Journal of Nonlinear Dynamics*, pp. 194–207, 1994.

[44] Lankarani, H.M., and Nikravsh, P.E., "A contact force model with hysteresis damping for impact analysis of multibody systems," *Journal of Mechanical Design*, vol. 112, pp. 369–376, 1990.

[45] Love, A. E., *A treatise on the Mathematical Theory of Elasticity*. Dover Publishers, 4th ed., 1944.